



Fermi National Accelerator Laboratory

FERMILAB Conf-96/278-E
DØ

**Color Coherence in $p\bar{p}$ Collisions
at $\sqrt{s} = 1.8$ TeV**

S. Abachi et al.
The DØ Collaboration

*Fermi National Accelerator Laboratory
P.O. Box 500, Batavia, Illinois 60510-0500*

September 1996

Submitted to the *28th International Conference on High Energy Physics, Warsaw, Poland, July 25-31, 1996.*

Disclaimer

This report was prepared as an account of work sponsored by an agency of the United States Government. Neither the United States Government nor any agency thereof, nor any of their employees, makes any warranty, express or implied, or assumes any legal liability or responsibility for the accuracy, completeness or usefulness of any information, apparatus, product or process disclosed, or represents that its use would not infringe privately owned rights. Reference herein to any specific commercial product, process or service by trade name, trademark, manufacturer or otherwise, does not necessarily constitute or imply its endorsement, recommendation or favoring by the United States Government or any agency thereof. The views and opinions of authors expressed herein do not necessarily state or reflect those of the United States Government or any agency thereof.

Distribution

Approved for public release: further dissemination unlimited.

Color Coherence in $p\bar{p}$ Collisions

at $\sqrt{s} = 1.8$ TeV

The DØ Collaboration*

(July 1996)

Abstract

We report on two preliminary studies of color coherence effects in $p\bar{p}$ collisions based on data collected by the DØ detector during the 1992–1993 and 1994–1995 runs of the Fermilab Tevatron collider at a center of mass energy $\sqrt{s} = 1.8$ TeV. Demonstration of initial-to-final state color interference effects is done in a higher energy region by measuring spatial correlations between the softer third jet and the second leading- E_T jet in multi-jet events and in a lower energy regime by examining particle distribution patterns in W +Jet events. The data are compared to Monte Carlo simulations with different color coherence implementations and to the predictions of a NLO parton level calculation.

S. Abachi,¹⁴ B. Abbott,²⁸ M. Abolins,²⁵ B.S. Acharya,⁴³ I. Adam,¹² D.L. Adams,³⁷
M. Adams,¹⁷ S. Ahn,¹⁴ H. Aihara,²² J. Alitti,⁴⁰ G. Álvarez,¹⁸ G.A. Alves,¹⁰

*Submitted to the 28th International Conference on High Energy Physics, Warsaw, Poland, 25-31 July 1996.

E. Amidi,²⁹ N. Amos,²⁴ E.W. Anderson,¹⁹ S.H. Aronson,⁴ R. Astur,⁴²
R.E. Avery,³¹ M.M. Baarmand,⁴² A. Baden,²³ V. Balamurali,³² J. Balderston,¹⁶
B. Baldin,¹⁴ S. Banerjee,⁴³ J. Bantly,⁵ J.F. Bartlett,¹⁴ K. Bazizi,³⁹ J. Bendich,²²
S.B. Beri,³⁴ I. Bertram,³⁷ V.A. Bezzubov,³⁵ P.C. Bhat,¹⁴ V. Bhatnagar,³⁴
M. Bhattacharjee,¹³ A. Bischoff,⁹ N. Biswas,³² G. Blazey,¹⁴ S. Blessing,¹⁵
P. Bloom,⁷ A. Boehnlein,¹⁴ N.I. Bojko,³⁵ F. Borcharding,¹⁴ J. Borders,³⁹
C. Boswell,⁹ A. Brandt,¹⁴ R. Brock,²⁵ A. Bross,¹⁴ D. Buchholz,³¹ V.S. Burtovoi,³⁵
J.M. Butler,³ W. Carvalho,¹⁰ D. Casey,³⁹ H. Castilla-Valdez,¹¹ D. Chakraborty,⁴²
S.-M. Chang,²⁹ S.V. Chekulaev,³⁵ L.-P. Chen,²² W. Chen,⁴² S. Choi,⁴¹
S. Chopra,²⁴ B.C. Choudhary,⁹ J.H. Christenson,¹⁴ M. Chung,¹⁷ D. Claes,⁴²
A.R. Clark,²² W.G. Cobau,²³ J. Cochran,⁹ W.E. Cooper,¹⁴ C. Cretsinger,³⁹
D. Cullen-Vidal,⁵ M.A.C. Cummings,¹⁶ D. Cutts,⁵ O.I. Dahl,²² K. De,⁴⁴
M. Demarteau,¹⁴ N. Denisenko,¹⁴ D. Denisov,¹⁴ S.P. Denisov,³⁵ H.T. Diehl,¹⁴
M. Diesburg,¹⁴ G. Di Loreto,²⁵ R. Dixon,¹⁴ P. Draper,⁴⁴ J. Drinkard,⁸ Y. Ducros,⁴⁰
S.R. Dugad,⁴³ D. Edmunds,²⁵ J. Ellison,⁹ V.D. Elvira,⁴² R. Engelmann,⁴² S. Eno,²³
G. Eppley,³⁷ P. Ermolov,²⁶ O.V. Eroshin,³⁵ V.N. Evdokimov,³⁵ S. Fahey,²⁵
T. Fahland,⁵ M. Fatyga,⁴ M.K. Fatyga,³⁹ J. Featherly,⁴ S. Feher,¹⁴ D. Fein,²
T. Ferbel,³⁹ G. Finocchiaro,⁴² H.E. Fisk,¹⁴ Y. Fisyak,⁷ E. Flattum,²⁵ G.E. Forden,²
M. Fortner,³⁰ K.C. Frame,²⁵ P. Franzini,¹² S. Fuess,¹⁴ E. Gallas,⁴⁴ A.N. Galyaev,³⁵
T.L. Geld,²⁵ R.J. Genik II,²⁵ K. Genser,¹⁴ C.E. Gerber,¹⁴ B. Gibbard,⁴
V. Glebov,³⁹ S. Glenn,⁷ J.F. Glicenstein,⁴⁰ B. Gobbi,³¹ M. Goforth,¹⁵
A. Goldschmidt,²² B. Gómez,¹ G. Gomez,²³ P.I. Goncharov,³⁵
J.L. González Solís,¹¹ H. Gordon,⁴ L.T. Goss,⁴⁵ N. Graf,⁴ P.D. Grannis,⁴²
D.R. Green,¹⁴ J. Green,³⁰ H. Greenlee,¹⁴ G. Griffin,⁸ N. Grossman,¹⁴
P. Grudberg,²² S. Grünendahl,³⁹ W.X. Gu,^{14,*} G. Guglielmo,³³ J.A. Guida,²
J.M. Guida,⁵ W. Guryn,⁴ S.N. Gurzhiev,³⁵ P. Gutierrez,³³ Y.E. Gutnikov,³⁵
N.J. Hadley,²³ H. Haggerty,¹⁴ S. Hagopian,¹⁵ V. Hagopian,¹⁵ K.S. Hahn,³⁹

R.E. Hall,⁸ S. Hansen,¹⁴ R. Hatcher,²⁵ J.M. Hauptman,¹⁹ D. Hedin,³⁰
 A.P. Heinson,⁹ U. Heintz,¹⁴ R. Hernández-Montoya,¹¹ T. Heuring,¹⁵ R. Hirosky,¹⁵
 J.D. Hobbs,¹⁴ B. Hoeneisen,^{1,†} J.S. Hoftun,⁵ F. Hsieh,²⁴ Tao Hu,^{14,*} Ting Hu,⁴²
 Tong Hu,¹⁸ T. Huehn,⁹ S. Igarashi,¹⁴ A.S. Ito,¹⁴ E. James,² J. Jaques,³²
 S.A. Jerger,²⁵ J.Z.-Y. Jiang,⁴² T. Joffe-Minor,³¹ H. Johari,²⁹ K. Johns,²
 M. Johnson,¹⁴ H. Johnstad,²⁹ A. Jonckheere,¹⁴ M. Jones,¹⁶ H. Jöstlein,¹⁴
 S.Y. Jun,³¹ C.K. Jung,⁴² S. Kahn,⁴ G. Kalbfleisch,³³ J.S. Kang,²⁰ R. Kehoe,³²
 M.L. Kelly,³² L. Kerth,²² C.L. Kim,²⁰ S.K. Kim,⁴¹ A. Klatchko,¹⁵ B. Klima,¹⁴
 B.I. Klochkov,³⁵ C. Klopfenstein,⁷ V.I. Klyukhin,³⁵ V.I. Kochetkov,³⁵ J.M. Kohli,³⁴
 D. Koltick,³⁶ A.V. Kostritskiy,³⁵ J. Kotcher,⁴ J. Kourlas,²⁸ A.V. Kozelov,³⁵
 E.A. Kozlovski,³⁵ M.R. Krishnaswamy,⁴³ S. Krzywdzinski,¹⁴ S. Kunori,²³
 S. Lami,⁴² G. Landsberg,¹⁴ J-F. Lebrat,⁴⁰ A. Leflat,²⁶ H. Li,⁴² J. Li,⁴⁴ Y.K. Li,³¹
 Q.Z. Li-Demarteau,¹⁴ J.G.R. Lima,³⁸ D. Lincoln,²⁴ S.L. Linn,¹⁵ J. Linnemann,²⁵
 R. Lipton,¹⁴ Y.C. Liu,³¹ F. Lobkowicz,³⁹ S.C. Loken,²² S. Lököš,⁴² L. Lueking,¹⁴
 A.L. Lyon,²³ A.K.A. Maciel,¹⁰ R.J. Madaras,²² R. Madden,¹⁵
 L. Magaña-Mendoza,¹¹ S. Mani,⁷ H.S. Mao,^{14,*} R. Markeloff,³⁰ L. Markosky,²
 T. Marshall,¹⁸ M.I. Martin,¹⁴ B. May,³¹ A.A. Mayorov,³⁵ R. McCarthy,⁴²
 T. McKibben,¹⁷ J. McKinley,²⁵ T. McMahon,³³ H.L. Melanson,¹⁴
 J.R.T. de Mello Neto,³⁸ K.W. Merritt,¹⁴ H. Miettinen,³⁷ A. Mincer,²⁸
 J.M. de Miranda,¹⁰ C.S. Mishra,¹⁴ N. Mokhov,¹⁴ N.K. Mondal,⁴³
 H.E. Montgomery,¹⁴ P. Mooney,¹ H. da Motta,¹⁰ M. Mudan,²⁸ C. Murphy,¹⁷
 F. Nang,⁵ M. Narain,¹⁴ V.S. Narasimham,⁴³ A. Narayanan,² H.A. Neal,²⁴
 J.P. Negret,¹ E. Neis,²⁴ P. Nemethy,²⁸ D. Nešić,⁵ M. Nicola,¹⁰ D. Norman,⁴⁵
 L. Oesch,²⁴ V. Oguri,³⁸ E. Oltman,²² N. Oshima,¹⁴ D. Owen,²⁵ P. Padley,³⁷
 M. Pang,¹⁹ A. Para,¹⁴ C.H. Park,¹⁴ Y.M. Park,²¹ R. Partridge,⁵ N. Parua,⁴³
 M. Paterno,³⁹ J. Perkins,⁴⁴ A. Peryshkin,¹⁴ M. Peters,¹⁶ H. Piekarz,¹⁵
 Y. Pischalnikov,³⁶ V.M. Podstavkov,³⁵ B.G. Pope,²⁵ H.B. Prosper,¹⁵

S. Protopopescu,⁴ D. Pušeljčić,²² J. Qian,²⁴ P.Z. Quintas,¹⁴ R. Raja,¹⁴
 S. Rajagopalan,⁴² O. Ramirez,¹⁷ M.V.S. Rao,⁴³ P.A. Rapidis,¹⁴ L. Rasmussen,⁴²
 S. Reucroft,²⁹ M. Rijssenbeek,⁴² T. Rockwell,²⁵ N.A. Roe,²² P. Rubinov,³¹
 R. Ruchti,³² J. Rutherford,² A. Sánchez-Hernández,¹¹ A. Santoro,¹⁰ L. Sawyer,⁴⁴
 R.D. Schamberger,⁴² H. Schellman,³¹ J. Sculli,²⁸ E. Shabalina,²⁶ C. Shaffer,¹⁵
 H.C. Shankar,⁴³ R.K. Shivpuri,¹³ M. Shupe,² J.B. Singh,³⁴ V. Sirotenko,³⁰
 W. Smart,¹⁴ A. Smith,² R.P. Smith,¹⁴ R. Snihur,³¹ G.R. Snow,²⁷ J. Snow,³³
 S. Snyder,⁴ J. Solomon,¹⁷ P.M. Sood,³⁴ M. Sosebee,⁴⁴ M. Souza,¹⁰
 A.L. Spadafora,²² R.W. Stephens,⁴⁴ M.L. Stevenson,²² D. Stewart,²⁴
 D.A. Stoianova,³⁵ D. Stoker,⁸ K. Streets,²⁸ M. Strovink,²² A. Sznajder,¹⁰
 P. Tamburello,²³ J. Tarazi,⁸ M. Tartaglia,¹⁴ T.L. Taylor,³¹ J. Thompson,²³
 T.G. Trippe,²² P.M. Tuts,¹² N. Varelas,²⁵ E.W. Varnes,²² P.R.G. Virador,²²
 D. Vititoe,² A.A. Volkov,³⁵ A.P. Vorobiev,³⁵ H.D. Wahl,¹⁵ G. Wang,¹⁵
 J. Warchol,³² G. Watts,⁵ M. Wayne,³² H. Weerts,²⁵ A. White,⁴⁴ J.T. White,⁴⁵
 J.A. Wightman,¹⁹ J. Wilcox,²⁹ S. Willis,³⁰ S.J. Wimpenny,⁹ J.V.D. Wirjawan,⁴⁵
 J. Womersley,¹⁴ E. Won,³⁹ D.R. Wood,²⁹ H. Xu,⁵ R. Yamada,¹⁴ P. Yamin,⁴
 C. Yanagisawa,⁴² J. Yang,²⁸ T. Yasuda,²⁹ P. Yepes,³⁷ C. Yoshikawa,¹⁶ S. Youssef,¹⁵
 J. Yu,¹⁴ Y. Yu,⁴¹ Q. Zhu,²⁸ Z.H. Zhu,³⁹ D. Zieminska,¹⁸ A. Zieminski,¹⁸
 E.G. Zverev,²⁶ and A. Zylberstejn⁴⁰

¹Universidad de los Andes, Bogotá, Colombia

²University of Arizona, Tucson, Arizona 85721

³Boston University, Boston, Massachusetts 02215

⁴Brookhaven National Laboratory, Upton, New York 11973

⁵Brown University, Providence, Rhode Island 02912

⁶Universidad de Buenos Aires, Buenos Aires, Argentina

⁷University of California, Davis, California 95616

- ⁸University of California, Irvine, California 92717
- ⁹University of California, Riverside, California 92521
- ¹⁰LAFEX, Centro Brasileiro de Pesquisas Físicas, Rio de Janeiro, Brazil
- ¹¹CINVESTAV, Mexico City, Mexico
- ¹²Columbia University, New York, New York 10027
- ¹³Delhi University, Delhi, India 110007
- ¹⁴Fermi National Accelerator Laboratory, Batavia, Illinois 60510
- ¹⁵Florida State University, Tallahassee, Florida 32306
- ¹⁶University of Hawaii, Honolulu, Hawaii 96822
- ¹⁷University of Illinois at Chicago, Chicago, Illinois 60607
- ¹⁸Indiana University, Bloomington, Indiana 47405
- ¹⁹Iowa State University, Ames, Iowa 50011
- ²⁰Korea University, Seoul, Korea
- ²¹Kyungsung University, Pusan, Korea
- ²²Lawrence Berkeley National Laboratory and University of California, Berkeley, California 94720
- ²³University of Maryland, College Park, Maryland 20742
- ²⁴University of Michigan, Ann Arbor, Michigan 48109
- ²⁵Michigan State University, East Lansing, Michigan 48824
- ²⁶Moscow State University, Moscow, Russia
- ²⁷University of Nebraska, Lincoln, Nebraska 68588
- ²⁸New York University, New York, New York 10003
- ²⁹Northeastern University, Boston, Massachusetts 02115
- ³⁰Northern Illinois University, DeKalb, Illinois 60115
- ³¹Northwestern University, Evanston, Illinois 60208
- ³²University of Notre Dame, Notre Dame, Indiana 46556
- ³³University of Oklahoma, Norman, Oklahoma 73019
- ³⁴University of Panjab, Chandigarh 16-00-14, India

³⁵Institute for High Energy Physics, 142-284 Protvino, Russia

³⁶Purdue University, West Lafayette, Indiana 47907

³⁷Rice University, Houston, Texas 77251

³⁸Universidade Estadual do Rio de Janeiro, Brazil

³⁹University of Rochester, Rochester, New York 14627

⁴⁰CEA, DAPNIA/Service de Physique des Particules, CE-SACLAY, France

⁴¹Seoul National University, Seoul, Korea

⁴²State University of New York, Stony Brook, New York 11794

⁴³Tata Institute of Fundamental Research, Colaba, Bombay 400005, India

⁴⁴University of Texas, Arlington, Texas 76019

⁴⁵Texas A&M University, College Station, Texas 77843

I. INTRODUCTION

Color coherence phenomena have been observed in experiments [1–6] studying the angular flow of hadrons in three-jet events from e^+e^- annihilations, in what has been termed the “string” [7] or “drag” [8] effect. The particle population in the region between quark and antiquark jets in $e^+e^- \rightarrow q\bar{q}g$ events has been measured to be suppressed with respect to the region between (anti)quark and gluon jets. This asymmetry, in the language of perturbative QCD, arises from constructive and destructive interference among the soft gluons radiated from the q , \bar{q} , and g . While quantum mechanical interference effects are expected in QCD, it is of real importance that the experimental results demonstrate that such interference effects survive the hadronization process, a phenomenon which the authors of Ref. [8] call *Local Parton-Hadron Duality* (LPHD).

The study of hard processes in hadron-hadron collisions is more complicated, experimentally and theoretically, than in e^+e^- annihilation due to the

presence of colored constituents in both the initial and final states. In addition, any event-by-event fluctuations of the soft particles produced by the underlying event may complicate the experimental results further. During a hard interaction, color is transferred from one parton to another. Examples of color flow diagrams are shown in Figs. 1 and 2 for $q\bar{q}$ and qg scattering. In Fig. 1a ($q\bar{q}$) the color system in which interference occurs is entirely between initial and final state, whereas in Fig. 1b (qg) interference also occurs in the initial and final states due to their explicit color connection. Similarly, in the cases where a colorless W boson is produced in the final state, Fig. 2a ($q\bar{q}$) illustrates a color system in which interference occurs solely between the partons in the initial and final state, whereas in Fig. 2b (qg) the resulting interference is between initial states in addition to that between initial and final state. The color connected partons act as a color antenna. Bremsstrahlung gluon radiation associated with the incoming and the outgoing partons leads to the formation of jets of hadrons around the direction of these colored emitters. It is the interference of such emissions (to leading order in N_c , the number of colors) that give rise to the color coherence effects in perturbative QCD calculations [9,10].

An important consequence of color coherence is the *Angular Ordering* (AO) approximation of the sequential parton decays. To leading order in N_C , AO leads to a suppression of soft gluon radiation in certain regions of phase space. In the case of outgoing partons, AO reduces the available phase space to an angular-ordered region, in which the successive emission angles of soft gluons decrease as the partonic cascade evolves away from the hard process. Outside this angular-ordered region the interference of different emission diagrams becomes destructive and the azimuthally integrated amplitude vanishes to leading order. However, for the incoming partons, the emission angles increase as the process develops from the initial hadrons to the hard subprocess. Monte Carlo

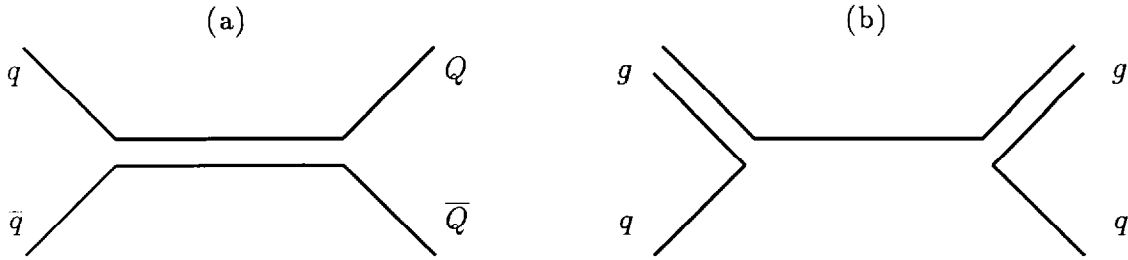


FIG. 1. Color flow diagrams for (a) $q\bar{q}$ and (b) qg scattering.

simulations including coherence via AO are available for both initial and final state evolutions [11,12]. While AO provides an approximate description of color coherence effects, QCD calculations taken to sufficiently high order should model the effects properly. Use of the latter approach, however, is limited, due to the current lack of higher-order calculations.

The DØ detector [13] with its hermetic uranium-liquid-argon calorimetry is especially suited for studying jet final states. Evidence has been reported [14–16] for color coherence effects between initial and final states in $p\bar{p}$ interactions by measuring spatial correlations between soft and leading- E_T jets in multi-jet events. In this paper we report updated results from this analysis and we explicitly examine the dependence of color coherence effects upon perturbative AO.

A new, complementary investigation is also reported here which is sensitive to both perturbative interference effects and the non-perturbative fragmentation process. It takes advantage of the sensitivity of the calorimetry by examining soft particle distributions in W +Jet events and provides additional evidence for color coherence interference between initial and final states. In the non-perturbative regime, these color coherence effects can be modeled by fragmentation schemes that account for color connections among partons, with

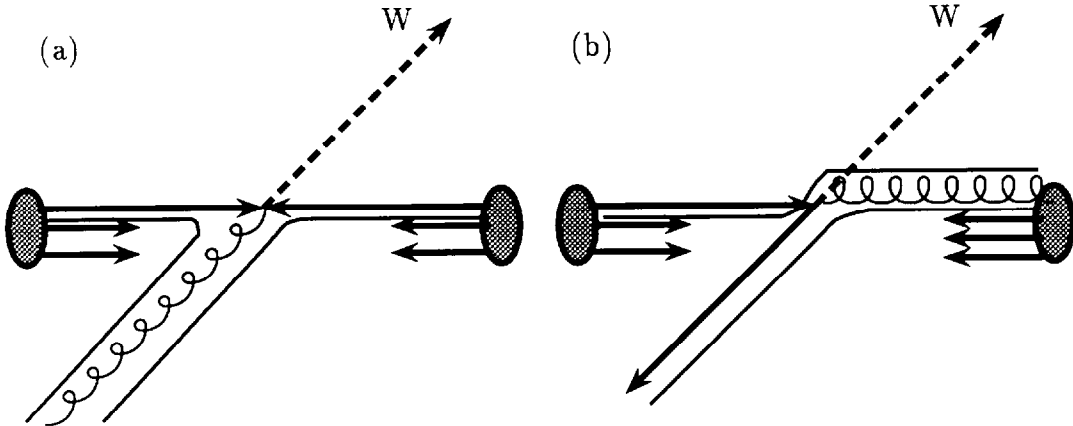


FIG. 2. Color flow diagrams for (a) $q\bar{q} \rightarrow Wg$ and (b) $qg \rightarrow Wq$. Thin solid lines represent the flow of color charge between the participating partons. Gluons are represented by helices.

results similar to perturbative angular ordering effects. This is the first time color coherence effects in $p\bar{p}$ interactions are studied using W bosons and jets.

In the following sections we describe the analysis procedures employed to study the color coherence effects in our multi-jet and W +Jet data samples.

II. METHOD OF ANALYSIS

A. Multi-jet Study

To minimize any complications caused by the underlying event fluctuations, events were selected such that the two leading jets had sufficiently high energies so that the coherent radiation formed secondary jets. The events were required to have three or more reconstructed jets. The jets were ordered in E_T and were labeled $E_{T1} > E_{T2} > E_{T3}$. The angular distribution, in (η, ϕ) space (where the pseudo-rapidity is defined as $\eta = -\ln(\tan(\frac{\theta}{2}))$), of the softer third

jet around the second highest- E_T jet was measured using the polar variables $R = \sqrt{(\Delta\eta)^2 + (\Delta\phi)^2}$ and $\beta = \tan^{-1}(\frac{\text{sign}(\eta_2) \cdot \Delta\phi}{\Delta\eta})$; where $\Delta\eta = \eta_3 - \eta_2$ and $\Delta\phi = \phi_3 - \phi_2$, in a search disk of $0.6 < R < \frac{\pi}{2}$ (Fig. 3). The expectation from initial-to-final state color interference is that the rate of soft jet emission around the event plane (i.e., the plane defined by the directions of the second jet and the beam axis) will be enhanced with respect to that around the transverse plane.

The data angular distributions are compared to particle shower level Monte Carlo simulations (ISAJET [17], HERWIG [11] and PYTHIA [12]) that differ in their implementation of color coherence. ISAJET uses an independent shower development model without any color coherence effects, HERWIG incorporates initial and final state interference effects by means of AO approximation of the parton cascades and PYTHIA also applies the AO approximation to the parton cascades but, in addition, uses string or independent fragmentation and allows the simulation of color coherence effects to be turned on or off while keeping the other properties of the generator the same. The data are also compared to the predictions of JETRAD [18]; a parton-level calculation consisting of the $\mathcal{O}(a_s^2) + \mathcal{O}(a_s^3)$ one-loop $2 \rightarrow 2$ parton scattering, combined together with the $\mathcal{O}(a_s^3)$ tree-level $2 \rightarrow 3$ scattering amplitudes.

B. W +Jet Study

Events with a W boson and opposing jet may also be used to study color coherence effects in hadronic collisions. In these events, the distribution of soft particles is measured around both the W boson and the opposing jet in order to observe interference effects. Since the W boson is a colorless object, it does not contribute to the production of secondary particles, thereby providing a template against which the pattern around the jet may be compared.

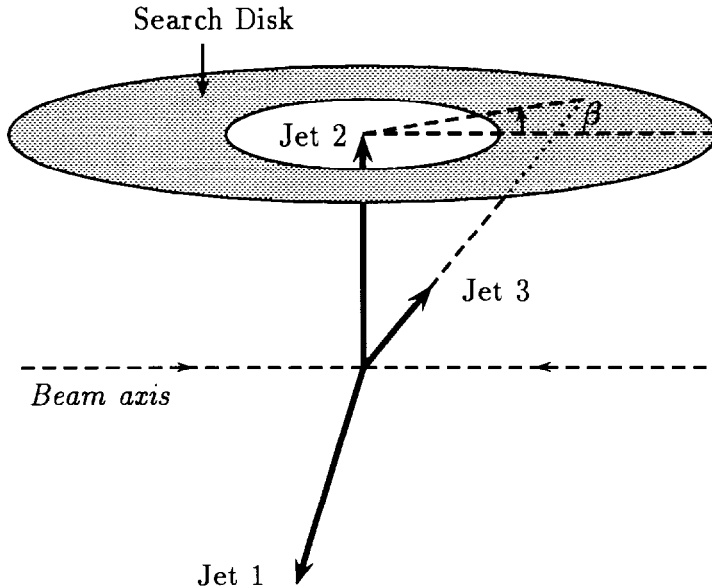


FIG. 3. Three-jet event topology illustrating the search disk (gray area) for studying the angular distribution of the softer third jet around the second leading- E_T jet.

This comparison serves to alleviate global detector and underlying event effects which are present in the vicinity of both the W boson and the jet.

The distribution of soft particles in the collider data is approximated in this analysis by measuring the distribution of projective calorimeter towers (columns of cells of area $\Delta\eta \times \Delta\phi = 0.1 \times 0.1$ radiating outward from the center of the detector) with $E_T > 250 \text{ MeV}$. This threshold was chosen in order to minimize contributions from low-energy calorimeter noise.

Events with the decay $W \rightarrow e + \nu$ are used in this analysis. The W boson is reconstructed from the decay products, resulting in a twofold ambiguity in the W boson rapidity (y_W) due to a similar ambiguity in the neutrino p_z . Monte Carlo studies have shown that the smaller $|y_W|$ is correct approximately 2/3 of the time, so this is the solution chosen. This choice is also made in the Monte Carlo W boson reconstruction to retain consistency in the comparison with

collider data.

Once the W boson direction has been determined in the detector, the opposing jet is tagged by selecting the highest- E_T jet in the ϕ hemisphere opposite to the W boson. Annular regions similar to those used in the multi-jet study are drawn around both the W boson and the jet in (η, ϕ) space, as shown in Fig. 4.

The angular distributions of towers above the 250MeV threshold are measured in these annular regions using the polar variables $R = \sqrt{(\Delta\eta)^2 + (\Delta\phi)^2}$ and $\beta_{W,Jet} = \tan^{-1}\left(\frac{\text{sign}(\eta_{W,Jet}) \cdot \Delta\phi_{W,Jet}}{\Delta\eta_{W,Jet}}\right)$; where $\Delta\eta_{W,Jet} = \eta_{Tower} - \eta_{W,Jet}$ and $\Delta\phi_{W,Jet} = \phi_{Tower} - \phi_{W,Jet}$, in a search disk of $0.7 < R < 1.5$. Similar to the multi-jet analysis, we expect the energetic tower distribution around the tagged jet to exhibit a depletion in the transverse plane relative to the event plane (when compared with the W boson distribution) due to initial-to-final state color interference.

The data angular distributions are compared to PYTHIA parton shower level Monte Carlo simulation with color coherence effects turned off and on with string and independent fragmentations. Furthermore, to determine the level of residual η -dependent detector effects in the measured patterns, minimum bias events are compared to the W +Jet data. In the minimum bias sample, locations for a fake W boson and fake jet are placed randomly in each event, with weights to reflect actual topological distributions in real W +Jet events. The analysis procedure is then applied to these events in order to observe the pattern of energetic towers in them. These patterns are compared with patterns in the real W +Jet data. Lastly, in order to minimize the statistical uncertainties in the W +jet sample, the annuli are folded about the ϕ symmetry axis, thereby reducing the β range to $0-\pi$.

III. EVENT SELECTION

A. Multi-jet Study

The data were collected during the 1992–1993 initial run of the DØ experiment. Events were selected using an inclusive jet trigger with E_T threshold of 85 GeV and pseudo-rapidity coverage of $|\eta| < 3.2$. The jets were reconstructed using a fixed-cone clustering algorithm with cone radius $R = \sqrt{(\Delta\eta)^2 + (\Delta\phi)^2} = 0.5$.

After jet energy scale corrections and jet quality cuts were applied, it was required that the transverse energy of the highest- E_T jet of the event be above 115 GeV to avoid any biases introduced by the trigger threshold. The interference effects were studied when the second leading- E_T jet was central ($|\eta_2| < 0.7$) or forward ($0.7 < |\eta_2| < 1.5$). The pseudo-rapidity of the leading jet was not explicitly constrained. The two leading jets were required to be in opposite ϕ hemispheres without imposing any tight back-to-back cut. The third jet was required to have $E_T > 15$ GeV.

B. W +Jet Study

The data were collected during the 1994–1995 run of the DØ experiment. Candidate $W \rightarrow e + \nu$ events were required to have at least one jet reconstructed using a fixed-cone clustering algorithm with cone radius $R = \sqrt{(\Delta\eta)^2 + (\Delta\phi)^2} = 0.7$. Both the electron and the event's missing E_T (\cancel{E}_T) were required to be greater than 25 GeV.

After electron and jet quality cuts were applied, the rapidity of the W boson was restricted to $|y_W| < 0.5$ and the jet pseudo-rapidity to $|\eta_{Jet}| < 0.5$. The W boson and the jet were only required to be in opposite ϕ hemispheres.

Additionally, the z component of the event vertex is restricted to $|z_{vtx}| < 20\text{cm}$ to retain the projective nature of the calorimeter towers.

IV. RESULTS

A. Multi-jet Study

The preliminary data β distributions along with Monte Carlo predictions are shown in Figs. 5 and 6. The HERWIG, ISAJET and PYTHIA simulations have been performed at the particle level, whereas the JETRAD predictions are at the parton level. Detector position and energy resolution effects have been included in all Monte Carlo predictions. The Monte Carlo events were subsequently processed using the same criteria employed for analyzing the data.

Figure 7 shows the ratios of the β distributions for the $D\bar{D}$ data relative to the several Monte Carlo predictions for both central ($|\eta_2| < 0.7$) and forward ($0.7 < |\eta_2| < 1.5$) regions. The absence of color interference effects in ISAJET results in a disagreement with the $D\bar{D}$ data distributions. The data show a clear excess of events compared to ISAJET near the event plane ($\beta = 0, \pi, 2\pi$) and a depletion at the transverse plane ($\beta = \frac{\pi}{2}, \frac{3\pi}{2}$), as expected from initial-to-final state coherent radiation effects. However, HERWIG which contains initial and final state interference effects implemented by means of an Angular Ordering (AO) approximation of the parton cascade, agrees well with the data. The $D\bar{D}$ data have also been compared to PYTHIA which also simulates the color interference effects with the AO approximation. From the DATA/PYTHIA comparisons we see that when we turn off the color coherence effects, PYTHIA disagrees with the data, whereas, it agrees better when the coherence effects are turned on with the other properties of the simulator being the same. Lastly, the $\mathcal{O}(a_s^3)$ tree-level QCD describes the coherence effects seen in data reasonably

well as shown by the DATA/JETRAD comparisons.

B. W +Jet Study

The preliminary azimuthally folded β distributions for the data are shown in Fig. 8. The number of towers above threshold is greater for the jet than for the W boson and the excess is enhanced in the event plane ($\beta = 0, \pi$) and minimized in the transverse plane ($\beta = \frac{\pi}{2}$), consistent with the expected trends of interference from color coherence effects. The errors include only statistical uncertainties, and systematic uncertainties based on the effects of calorimeter noise, energy smearing and multiple $p\bar{p}$ collisions have not been included in this measurement.

Ratios of the data tower distributions for the jet annular region relative to the W boson annulus are shown in Fig. 9 for W +jet minimum bias data. When compared to minimum bias data, W +Jet data show a significant enhancement in the event plane while approximately agreeing near the transverse plane, where constructive interference from initial-final state color coherence is at a minimum. In Fig. 10, PYTHIA with AO on and string fragmentation processed at the particle level is in qualitative agreement with the W +Jet data, exhibiting a similarly shaped curve, whereas when AO is turned off while using independent fragmentation it is in disagreement with the data.

V. CONCLUSIONS

Color coherence effects between initial and final states in $p\bar{p}$ interactions have been observed and studied in two analyses by the $D\bar{O}$ collaboration. Using multi-jet events we measured the spatial correlations between the second and the third leading- E_T jets and, by comparing the data distributions to sev-

eral MC predictions with different CC implementations, we were able to single out the initial-to-final state interference effects. Monte Carlo simulations that implement color interference effects by means of the AO approximation reproduce the data angular distributions reasonably well, with HERWIG best representing the data. Furthermore, preliminary results indicate that coherence effects as predicted by a $2 \rightarrow 3$ parton level calculation are also in agreement with the data.

We also presented the first preliminary results on color coherence effects in W +Jet events. Data show an enhancement of soft particle radiation in the event plane with respect to the transverse plane which is qualitatively consistent with PYTHIA predictions using the AO approximation and string fragmentation.

ACKNOWLEDGMENTS

We thank the staffs at Fermilab and the collaborating institutions for their contributions to the success of this work, and acknowledge support from the Department of Energy and National Science Foundation (U.S.A.), Commissariat à l'Énergie Atomique (France), Ministries for Atomic Energy and Science and Technology Policy (Russia), CNPq (Brazil), Departments of Atomic Energy and Science and Education (India), Colciencias (Colombia), CONACyT (Mexico), Ministry of Education and KOSEF (Korea), CONICET and UBACyT (Argentina), and the A.P. Sloan Foundation.

REFERENCES

- * Visitor from IHEP, Beijing, China.
- * Visitor from Univ. San Francisco de Quito, Ecuador.
- [1] W. Bartel *et al.* (JADE Collaboration), Phys. Lett. **B101**, 129 (1981);
Zeit. Phys. **C21**, 37 (1983); Phys. Lett. **B134**, 275 (1984).
- [2] H. Aihara *et al.* (TPC/ 2γ Collaboration), Phys. Rev. Lett. **54**, 270 (1985);
Zeit. Phys. **C28**, 31 (1985); Phys. Rev. Lett. **57**, 945 (1986).
- [3] M. Althoff *et al.* (TASSO Collaboration), Zeit. Phys. **C29**, 29 (1985).
- [4] P.D. Sheldon *et al.* (MARK2 Collaboration), Phys. Rev. Lett. **57**, 1398
(1986).
- [5] M.Z. Akrawy *et al.* (OPAL Collaboration), Phys. Lett. **B247**, 617 (1990);
Phys. Lett. **B261**, 334 (1991); P.D. Acton *et al.* Phys. Lett. **B287**, 401
(1992); Zeit. Phys. **C58**, 207 (1993).
- [6] M. Acciarri *et al.* (L3 Collaboration), CERN-PPE/95-49 (1995); submitted
to Phys. Lett. B.
- [7] B. Andersson, G. Gustafson, and T. Sjöstrand, Phys. Lett. **B94**, 211
(1980).
- [8] Ya.I. Azimov, Yu.L. Dokshitzer, V.A. Khoze, and S.I. Troyan, Phys. Lett.
B165, 147 (1985); Sov. Journ. Nucl. Phys. **43**, 95 (1986).
- [9] R.K. Ellis, G. Marchesini, and B.R. Webber, Nucl. Phys. **B286**, 643
(1987).
- [10] Yu.L. Dokshitzer, V.A. Khoze, A.H. Mueller, and S.I. Troyan, Basics of
Perturbative QCD, Editions Frontières (1991); Rev. Mod. Phys. **60**, 373

(1988).

- [11] G. Marchesini and B.R. Webber, Nucl. Phys. **B310**, 461 (1988).
- [12] H.-U. Bengtsson and T. Sjöstrand, Computer Physics Commun. **46** (1987) 43
- [13] S. Abachi *et al.* (DØ Collaboration), Nucl. Instr. Meth. **A338**, 185 (1994).
- [14] F. Borchering (DØ Collaboration), Proceedings of the 9th Topical Workshop on Proton-Antiproton Collider Physics, Tsukuba, Japan, 218, 18–22 Oct. 1993.
- [15] S. Abachi *et al.* (DØ Collaboration), Fermilab-Conf-95/182-E.
- [16] F. Abe *et al.* (CDF Collaboration), Phys. Rev. **D50**, 5562 (1994).
- [17] F.E. Paige and S.D. Protopopescu, BNL report No. 38034 (1986).
- [18] W.T. Giele, E.W.N. Glover, and D.A. Kosower, Phys. Rev. **D46**, 1980 (1992); Nucl. Phys. **B403**, 633 (1993); Phys. Rev. Lett. **73**, 2019 (1994).

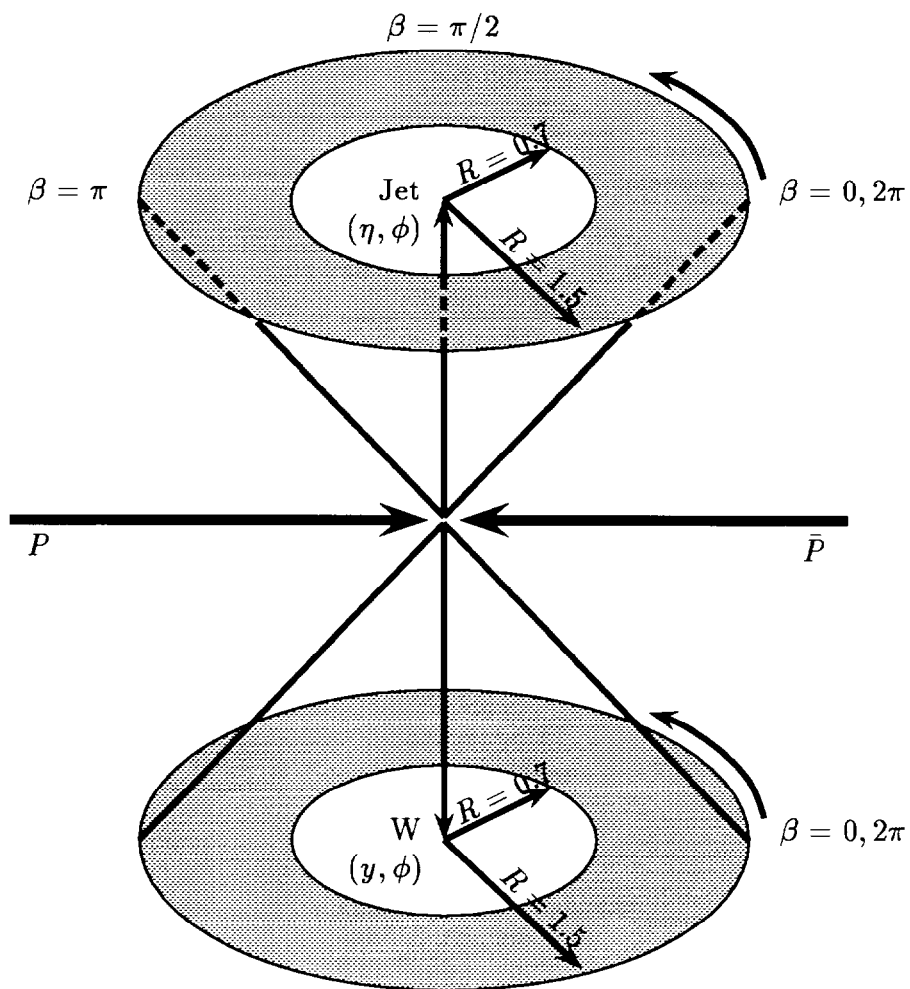


FIG. 4. W +Jet event topology illustrating the annuli and variables for studying the particle flow around the W boson and the leading- E_T jet in the opposite ϕ hemisphere.

DO PRELIMINARY

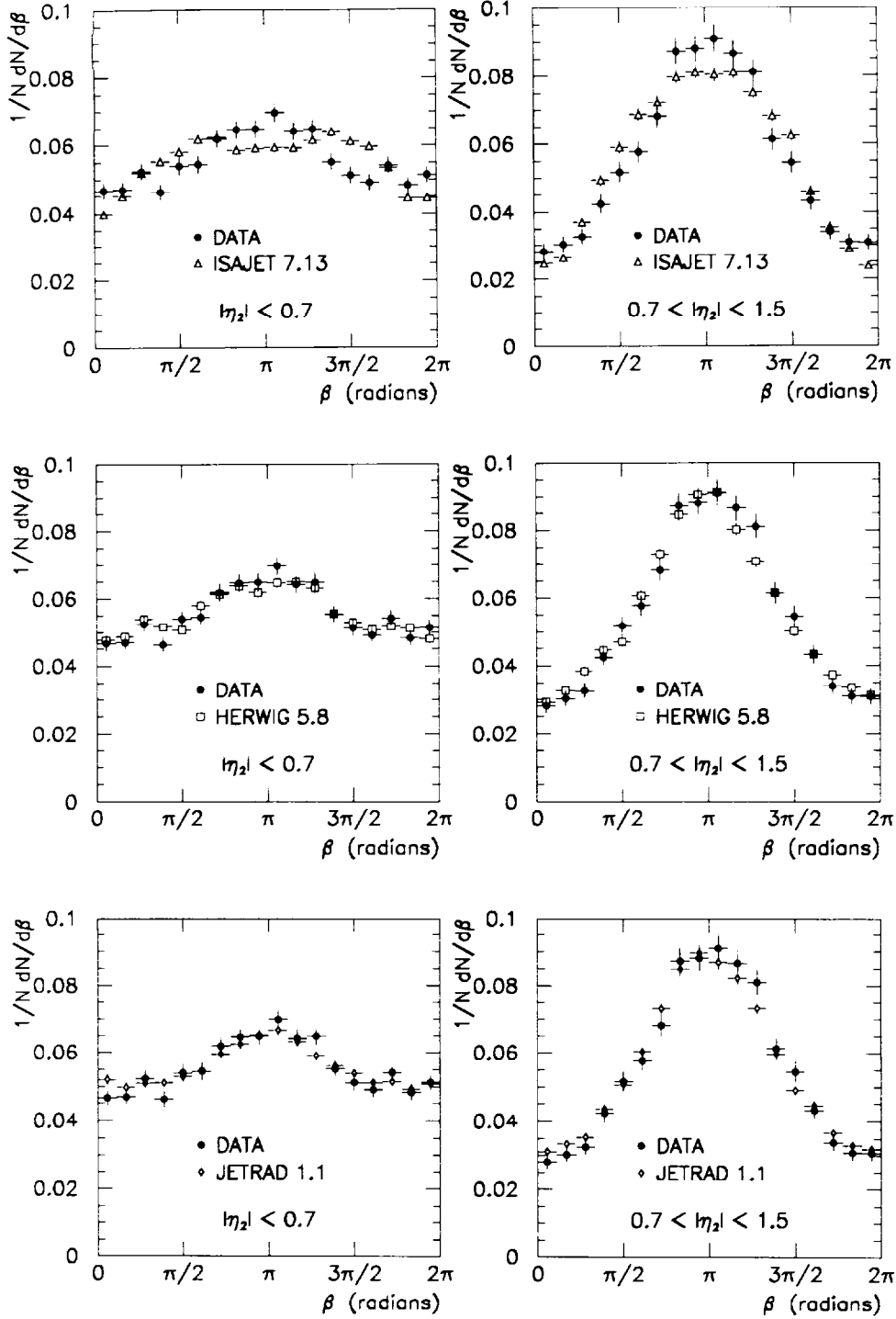


FIG. 5. Comparisons of the data β distributions for central ($|\eta_2| < 0.7$) and forward ($0.7 < |\eta_2| < 1.5$) jets to the predictions of HERWIG, ISAJET, and JETRAD. The error bars shown include statistical errors only.

DO PRELIMINARY

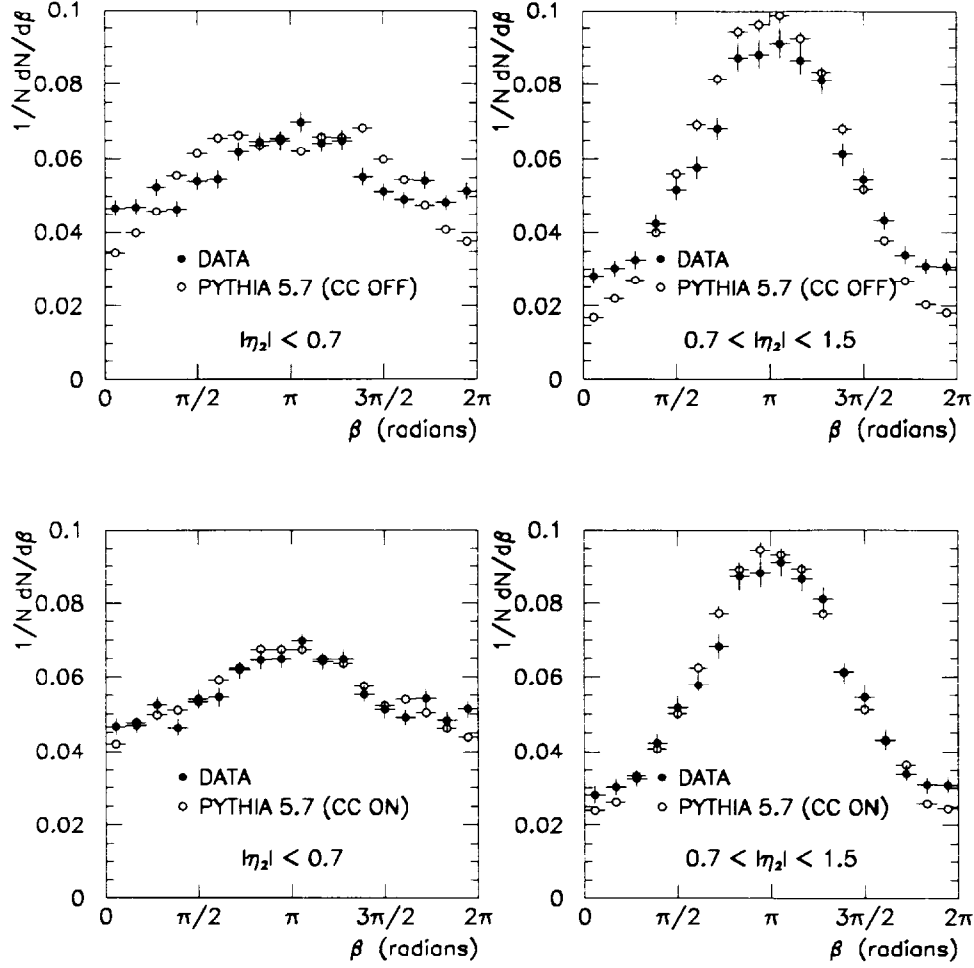


FIG. 6. Comparisons of the data β distributions for central ($|\eta_2| < 0.7$) and forward ($0.7 < |\eta_2| < 1.5$) jets to the predictions of PYTHIA, with coherence effects turned off and on. The error bars shown include statistical errors only.

D0 PRELIMINARY

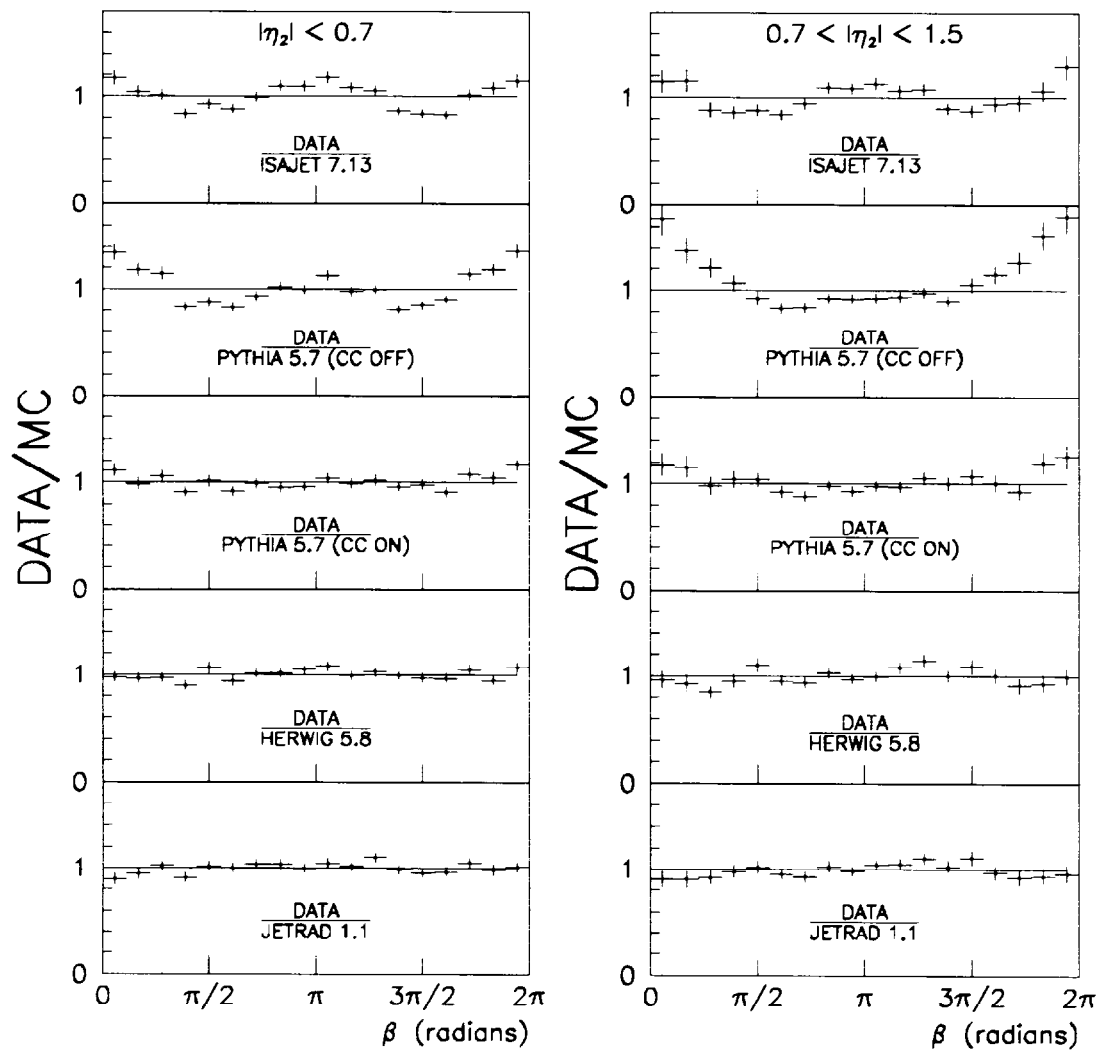


FIG. 7. Ratio of β distributions between data and Monte Carlo predictions for both central and forward pseudo-rapidity regions.

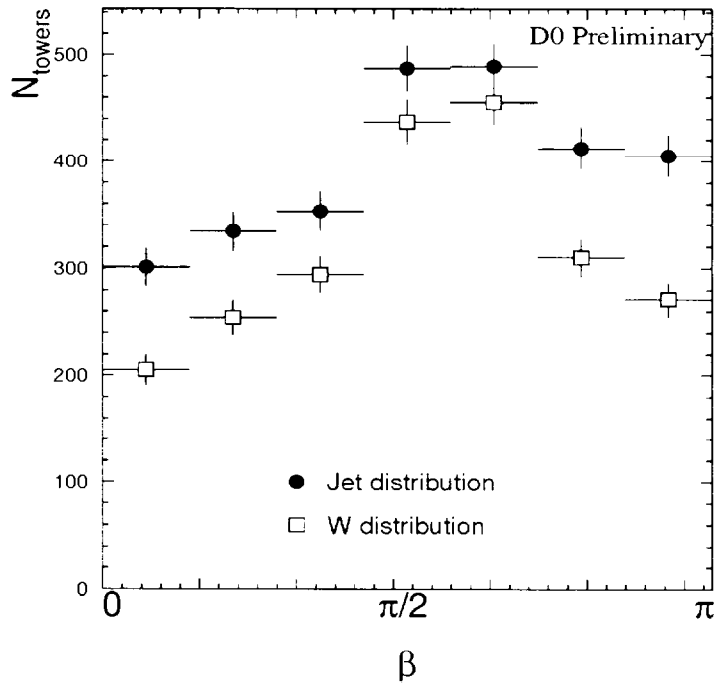


FIG. 8. Comparison of the data azimuthally folded β distributions around the jet (filled circles) and the W boson (open squares) for W +Jet events. The error bars shown include statistical errors only.

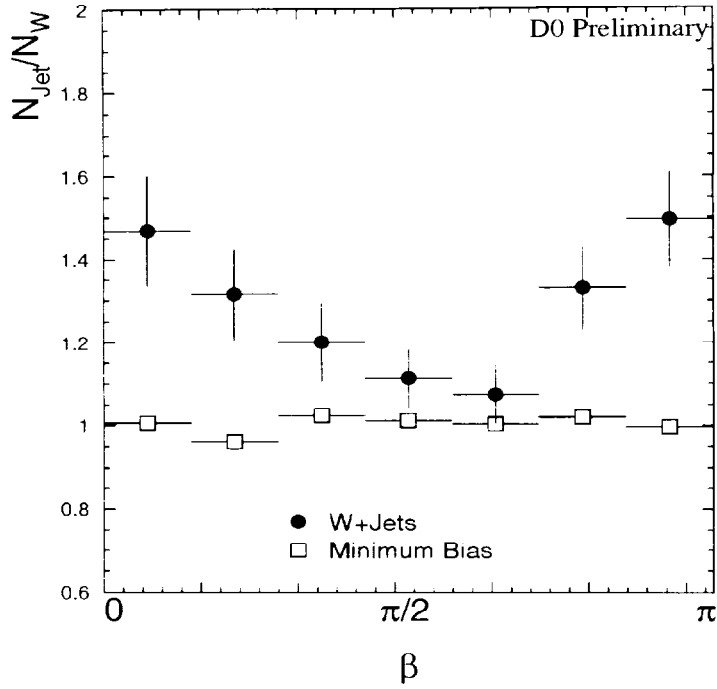


FIG. 9. Ratios of data folded β distributions between the jet and the W boson for W +Jet data (filled circles) and for minimum bias data (open squares). The error bars shown include statistical errors only.

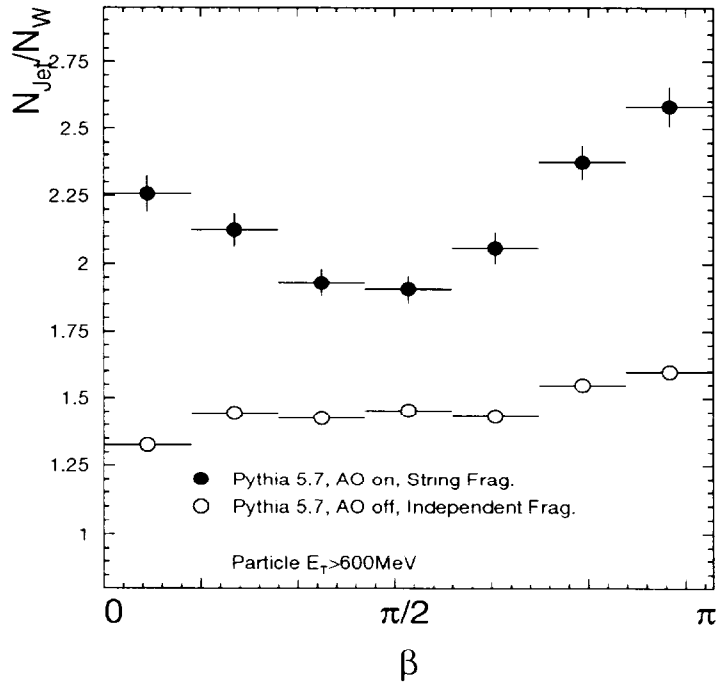


FIG. 10. Ratios of PYTHIA folded β distributions between the jet and the W boson for W +Jet events at the particle level with angular ordering on and string fragmentation (filled circles) and with angular ordering off and independent fragmentation (open circles). The error bars shown include statistical errors only.